Environmental Modelling & Software 60 (2014) 219–227

Contents lists available at ScienceDirect

Environmental Modelling & Software

journal homepage: www.elsevier.com/locate/envsoft

Uncertainty and sensitivity analyses using GLUE when modeling inhibition and pharmaceutical cometabolism during nitrification

Sandeep Sathyamoorthy, Richard M. Vogel, Steven C. Chapra, C. Andrew Ramsburg*

Tufts University, Department of Civil and Environmental Engineering, 200 College Avenue, Room 113 Anderson Hall, Medford, MA 02155, USA

ARTICLE INFO

Article history:
Received 1 August 2013
Received in revised form
15 May 2014
Accepted 7 June 2014
Available online

Keywords:
Activated sludge
Inhibition
Pharmaceutical
Ammonia
Elasticity
Structural error

ABSTRACT

The influence of uncertainties in biokinetic parameters for ammonia and nitrite oxidizing bacteria on the performance of a two-step nitrification model was evaluated using the Generalized Uncertainty Estimation (GLUE) technique. The predictive capability of behavioral simulations generated using GLUE was assessed utilizing data from experiments comparing nitrification in the presence and absence of two pharmaceuticals – atenolol or sotalol. Results suggest that GLUE cannot account for model structural error arising when ammonia oxidation is competitively inhibited. Use of a competitive inhibition model for ammonia oxidation (i.e., correction of the model structural error), however, enables GLUE to generate meaningful uncertainty intervals. While GLUE is used in the present study, other uncertainty analysis techniques are likely to be similarly unable to account for model structural errors. Thus, results from this study emphasize the importance of model selection for efficacious uncertainty analysis. The behavioral simulations generated using GLUE based on application of the correct model was subsequently used to evaluate the sensitivity of transformation coefficients employed to describe the cometabolism of atenolol by ammonia oxidizing bacteria (AOB). Sensitivity was assessed by computing nonparametric elasticities of the cometabolism transformation coefficients to biokinetic parameters selected to describe nitrification in a novel application of a generalized nonparametric analysis. Results suggest that the AOB-growth related transformation coefficient of atenolol is relatively insensitive to variation in ammonia and nitrite oxidizing biokinetic parameters. In contrast, the non-growth related transformation coefficient describing atenolol cometabolism appears to be sensitive to the specific growth rate of AOB. Elasticities are used to assess whether estimates of atenolol-AOB cometabolic biodegradation coefficients from lab-scale experiments could be used more generally. This novel application of elasticities to biological wastewater process modeling suggests that seasonal temperature variations may be an important factor in pharmaceutical biodegradation during biological wastewater treatment.

1. Introduction

The unified activated sludge model (ASM) framework has been extensively used for wastewater treatment process modeling since its development by the International Water Association task group (Henze et al., 2000). One of the reasons for the success of the ASM framework is its adaptability – the framework allows new descriptions of processes to be easily incorporated into the model structure, albeit at the expense of simplicity. The original ASM1 model had eight processes, thirteen components and nineteen parameters (Henze et al., 1987). In comparison, a recent updated model proposed by Hiatt and Grady (2008) relies on 18 processes, 20 components and 54 parameters. While some parameters are easily transferable from one system to another, application of the ASM model typically requires a significant number of assumptions related to biokinetics (e.g., maximum specific growth rates and half saturation values) and wastewater composition (e.g., COD fractionation). Understanding the uncertainty and sensitivity related to these assumptions is critical for the meaningful application of ASM in complex dynamic biological systems (Rieger et al., 2013). Both confidence intervals (associated with uncertainties in model parameters) and prediction intervals (which further incorporate model error) are important considerations when using ASM in wastewater treatment process design. Yet, industrial process simulators, as well as many research studies using aspects of the ASM framework found in these simulators, do not adequately account for uncertainties in model inputs (Belia et al., 2009). Important exceptions to this generalization include recent studies which

* Corresponding author. Tel.: +1 617 627 4286.
E-mail address: andrew.ramsburg@tufts.edu (C.A. Ramsburg).

http://dx.doi.org/10.1016/j.envsoft.2014.06.006
1364-8152/

employ Monte Carlo (MC) analyses (Flores-Alsina et al., 2008; Benedetti et al., 2011), couple MC analyses with Global Sensitivity Analyses (Flores-Alsina et al. (2012) and apply the Generalized Likelihood Uncertainty Estimation (GLUE) technique (Mannina et al., 2010, 2011, 2012).

GLUE was developed over 20 years ago for hydrologic modeling problems by Beven and Binley (1992) as an extension to the Generalized Sensitivity Analysis method (Hornberger and Spear, 1981). It has since been extensively used in a wide range of environmental science and engineering applications including modeling fate of emerging pollutants (Vezzaro et al., 2012; Vezzaro and Mikkelsen, 2012) and wastewater treatment processes (Sin et al., 2005; Di Bella et al., 2008; Mannina et al., 2010; Mannina et al., 2012; Cosenza et al., 2013). Critical to the use of GLUE is the concept of equifinality. Equifinality acknowledges that many different model parameter combinations can result in plausible model outcomes (Beven and Binley, 1992; Freer et al., 1996; Beven and Freer, 2001). The attractiveness of the GLUE technique lies in its ease of application, coupled with the claim that there is no need for assumptions related to the probability distribution of the residuals. Furthermore, Beven and Binley (1992) suggest that use of GLUE comprehensively reflects all sources of error including that arising from: (i) model selection (i.e., model structural error); (ii) parameter uncertainty; and (iii) model calibration (i.e., model error). Use of the GLUE technique, however, has been severely criticized. For example, Stedinger et al. (2008), argue that use of GLUE without a formal specification of the probability distribution of model error will in general, lead to results not suitable for scientific work. They further argue against implementation of a user-selected behavioral threshold on the basis that this selection is arbitrary and is not necessary when a formal likelihood function is used within a Bayesian context. Formal likelihood functions, however, can be difficult to develop for models describing complex processes, and for this reason are often replaced with informal (i.e., arbitrary) likelihood functions based upon goodness-of-fit metrics (e.g., Freer et al., 1996).

While GLUE has been extensively used and examined within the hydrology community, its application in biological process modeling is relatively recent (e.g., Mannina et al., 2010, 2011, 2012). Scrutiny of its applicability for uncertainty analysis in biological process modeling remains limited. Such an examination is needed given that the use of GLUE within industrial process models may hold potential for communicating uncertainty in model outputs. Notably absent from the literature is an evaluation of the influence of model selection (model structural error) on uncertainty and sensitivity analysis outcomes when using GLUE to generate confidence intervals associated with fitted models. Assessing the influence of model selection is a particularly important area of research when applying GLUE with ASM given the flexibility of the ASM model framework to readily incorporate new or updated models. Many researchers contend that GLUE produces uncertainty intervals for model predictions which account for model structural error among other things (e.g., Beven and Binley, 1992; Beven and Freer, 2001; Beven et al., 2008; Vrugt et al., 2009). This is, perhaps, best evidenced by the Beven and Freer (2001) claim that "Any effects of model nonlinearity, covariation of parameter values and errors in model structure, input data or observed variable, which the simulations are compared, are handled implicitly within this procedure''. However, research specifically designed to rigorously evaluate this claim demonstrates that GLUE is unable to produce reasonable uncertainty intervals when applied with ill-posed models or with large unknown errors (Mantovan and Todini, 2006; Stedinger et al., 2008; Renard et al., 2010). Thus, model structural error create a serious impediment to efficacious model uncertainty analyses (Liu and Gupta, 2007; Tian et al., 2014). The importance of using a correctly defined model when conducting uncertainty analysis is not unique to applications of GLUE. Model structural errors are generally the most poorly understood and the most difficult errors to address; nevertheless, the influence of structural errors on model predictions can be far more detrimental than the influence of the errors associated with parameters or data (Carrera and Neuman, 1986; Abramowitz et al., 2006; Liu and Gupta, 2007). Our study aims to explore the influence of model structural error on uncertainty intervals derived from GLUE. The conclusions we reach concerning GLUE should apply to other uncertainty methods in the sense that we are not aware of any uncertainty methods which can meaningfully incorporate the influence of model structural error. Thus, our results related to coupling GLUE with ASM, may also help clarify the importance of mitigating model structural error within the context of both model uncertainty analysis and parameter sensitivity analysis.

The primary objective of this paper is to assess the effectiveness of GLUE in capturing uncertainties associated with assumed biokinetic parameters when using ASM modules that may also contain model structural errors. Focus is placed on a subset of the complete ASM framework describing nitrification using a two-step model and a new process that describes cometabolic pharmaceutical (PhAC) degradation by ammonia oxidizing bacteria (AOB). Uncertainty analyses build upon experimental data and mathematical models developed when evaluating the biodegradation of selected beta blockers during nitrification (Sathyamoorthy et al., 2013). Importantly, the selected experimental data sets provide an opportunity to evaluate the uncertainty intervals developed by applying GLUE. Thus, the research reported herein offers an important step toward considering uncertainty in industrial process model simulators based on the ASM framework (e.g., GPSx, Biowin, SIMBA, etc.). Moreover, should GLUE provide meaningful insights for these experiments, it could be applied with ASM to quantify uncertainty in complex biological systems.

2. Materials and methods

2.1. Description of experiments

The experimental data and mathematical model which form the base of the uncertainty evaluation described herein are detailed in Sathyamoorthy et al. (2013). In brief, batch experiments were conducted and modeled using the ASM framework to evaluate pharmaceutical degradation by a nitrification enrichment culture. Nitrification control experiments – reactors to which no pharmaceutical was added – were conducted in parallel using the same biomass seed as those reactors exposed to the pharmaceutical. These control reactors, therefore, provide an opportunity to independently assess the initial biomass concentrations of AOB and nitrite oxidizing bacteria (NOB) as is further explained below. The experimental matrix contained a second type of control – one in which ammonia oxidation was inhibited. These reactors therefore provide an opportunity to independently assess the role of heterotrophs in degrading the selected pharmaceuticals. Samples were collected from each reactor over the course of 25 h and analyzed for ammonia, nitrite, nitrate, and pharmaceutical concentrations (Sathyamoorthy et al., 2013).

2.2. Application of GLUE for uncertainty analysis of nitrification process modeling

The GLUE technique relies on the output of numerous MC simulations each conducted with input parameters selected at random from a particular distribution (uniform distributions of model input parameters are most commonly used). Model outputs are used to determine a value of the likelihood function, which is then compared to an arbitrarily selected threshold value. Simulations producing a likelihood function below the threshold are termed non-behavioral and discarded from future consideration, while those simulations producing a likelihood function greater than the threshold are termed behavioral, and retained to generate confidence intervals associated with behavioral models (Beven and Binley, 1992). Note that our study, like many others, found that the model errors exhibit an extremely complex stochastic structure including serial correlation, heteroscedasticity and nonnormality. For this reason, similar to hundreds of other studies using GLUE, we elected to employ GLUE with an informal likelihood function. As has been shown by others, such an informal statistical analysis cannot, in general, be expected to produce uncertainty intervals for model output which enclose observed data, even if the correct model structure is known *a priori* (Stedinger et al., 2008). While we do not advocate the routine use of GLUE with an informal likelihood function (due to

the lack of rigorous statistical support of this type of approach, see Mantovan and Todini, 2006; Stedinger et al., 2008), it is acknowledged that others suggest that this is acceptable (see summary in Beven et al., 2000) and many adopt the informal likelihood approach in application (e.g., Mannina et al., 2010, 2011; Vezzaro and Mikkelsen, 2012). Within this context, our experiments provide an important and relevant opportunity to explicitly examine the role of model structural error when attempting to generate meaningful uncertainty intervals for simulations of ammonia oxidation in the presence of emerging contaminants.

In this research, 2000 Monte Carlo (MC) simulations were used with the application of GLUE. The decision to employ 2000 MC simulations represents a balance between computational overhead and maximizing coverage of the parameter space as analyses conducted with 500 and 1000 MC simulations provided statistically similar results to those obtained using the 2000 simulations (Mann Whitney $p > 0.05$). AOB and NOB biokinetic parameters for each of the 2000 MC simulations were randomly selected using a Latin hypercube sampling method (McKay et al., 1979) from uniform distributions that span the range of literature values (see Fig. 1). These randomly selected nitrification biokinetic parameters were then used to fit initial biomass concentrations of AOB ($X_{AOB,t0}$) and NOB ($X_{NOB,t0}$) in a two-step nitrification model shown in Fig. 1 (Chandran and Smets, 2000; Hiatt and Grady, 2008) by minimizing the sum of square errors (SSE) between measured and predicted values of ammonia-nitrogen (S_{NH}), nitrite-nitrogen (S_{NO2}) and nitrate-nitrogen (S_{NO3}) concentrations in the nitrification control reactor. Fits of X_{AOBt0} and X_{NOBt0} were constrained between 1 and the COD equivalent of the measured reactor VSS concentration.

Goodness-of-fit metrics used for the informal likelihood function have typically been based on the sum of square residuals or the ratio of the sum of square residuals to the variance of the observed data (i.e., the Nash Sutcliffe Efficiency, NSE) (Beven and Binley, 1992; Freer et al., 1996; Mannina et al., 2011). In this research the likelihood function (L_M) for each Monte Carlo simulation was determined by equally weighting the NSE for S_{NH}, S_{NO2} and S_{NO3} for the model description of nitrification (Eq. (1)).

$$L_M(\theta_k|Y_k) = \frac{1}{3}\left(1 - \frac{\sigma^2_{e,S_{NH},k}}{\sigma^2_{o,S_{NH}}}\right) + \frac{1}{3}\left(1 - \frac{\sigma^2_{e,S_{NO2},k}}{\sigma^2_{o,S_{NO2}}}\right) + \frac{1}{3}\left(1 - \frac{\sigma^2_{e,S_{NO3},k}}{\sigma^2_{o,S_{NO3}}}\right) \quad (1)$$

where

for the kth simulation:
$\sigma^2_{e,S_{NH},k}$ = variance of the residuals for S_{NH};
$\sigma^2_{e,S_{NO2},k}$ = variance of the residuals for S_{NO2};
$\sigma^2_{e,S_{NO3},k}$ = variance of the residuals for S_{NO3};

for the experimental data:
$\sigma^2_{o,S_{NH}}$ = variance of the measured values of S_{NH};
$\sigma^2_{o,S_{NO2}}$ = variance of the measured values of S_{NO2};
$\sigma^2_{o,S_{NO3}}$ = variance of the measured values of S_{NO3}.

Each of the 2000 L_M values are compared with the behavioral threshold ($L_{M,BEV}$) in order to determine which simulations are behavioral and thus retained for the uncertainty analysis. As Beven and Binley (1992) and others have noted, the selection of $L_{M,BEV}$ is inherently subjective. However, the development of an L_M based upon NSE permits us to select a $L_{M,BEV}$ that is consistent with good model performance (e.g., NSE > 0.70, as recommended by McCuen et al., 2006; Moriasi et al., 2007). This criterion effectively ensures that the production of uncertainty intervals is based upon meaningful models which mimic important properties of the observations. Following rejection of the non-behavioral simulations, L_M values for the behavioral simulations are rescaled to produce $L_{M,UPDATED}$ such that $\sum L_{M,UPDATED} = 1$. The resulting behavioral simulations are sorted on the basis of $L_{M,UPDATED}$ and desired quantiles are selected. Uncertainty intervals are then developed by identifying those parameter sets that correspond to the 5th and 95th percentile values of $L_{M,UPDATED}$ for the nitrification control reactors.

2.3. Parameter sensitivity analyses

In addition to using GLUE for evaluating uncertainty intervals for model predictions, we also introduce and employ a novel sensitivity analysis technique that uses a nonparametric method to calculate parameter elasticity. Elasticity is a measure of the fractional change in an output variable given a fractional change in an input variable. While popular in economics, elasticity coefficients have been used in fields ranging from hydrology (Sankarasubramanian et al., 2001; Chiew, 2006) to biochemistry and metabolic engineering (Fell, 1992). Most approaches to estimation of elasticity are parametric, in the sense that they require several assumptions to enable their estimation. In contrast, our approach to estimation of elasticity coefficients is nonparametric because the method does not require any assumptions related to the form of the model structure. Rather, the method only uses the chain rule of differentiation.

Focus is placed on the atenolol data set as atenolol was the only beta blocker evaluated in our experiments that was observed to degrade during ammonia oxidation (Sathyamoorthy et al., 2013). Biodegradation of atenolol is described using a cometabolic process-based (CPB) model developed in Sathyamoorthy et al. (2013). Briefly, the CPB model (Eq. (2)) is based upon the integrated cometabolic biodegradation model proposed by Criddle (1993), and includes three biodegradation processes for atenolol (i) cometabolic biodegradation linked to AOB growth (ii)

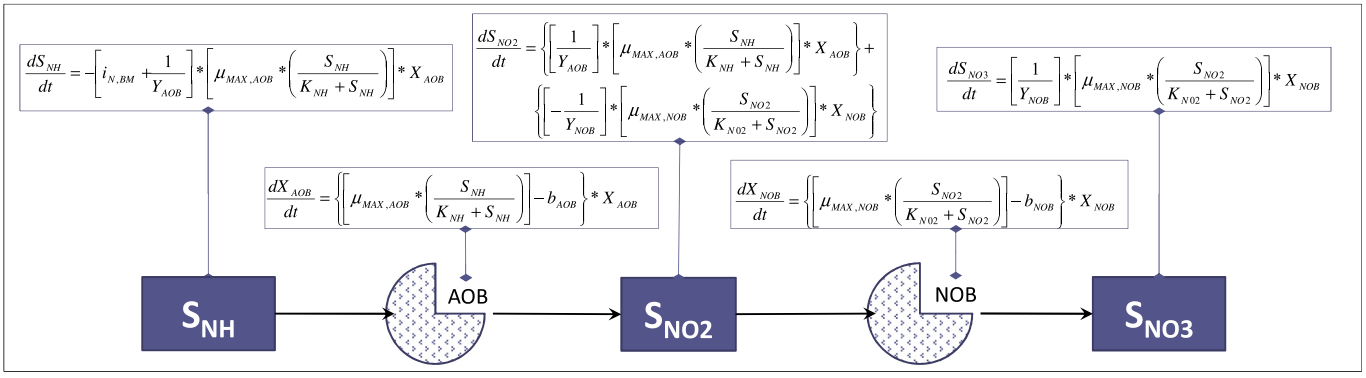

AOB biokinetic and stoichiometric parameters				
max. specific growth rate	$\mu_{max,AOB}$	(day^{-1})	0.2 – 1.6	(Munz et al., 2011)
decay rate	b_{AOB}	(day^{-1})	0.06 – 0.4	(Marsili-Libelli et al., 2001; Munz et al., 2011)
S_{NH} half saturation	K_{NH}	($mg\text{-}N{\cdot}L^{-1}$)	0.14 – 2.3	(Manser et al., 2005; Chandran et al., 2008)
S_{NH} yield	Y_{AOB}	($mg\text{-}COD{\cdot}mg\text{-}N^{-1}$)	0.11 – 0.21	(Hiatt and Grady, 2008; Sin et al., 2008; Munz et al., 2011)

NOB biokinetic and stoichiometric parameters				
max. specific growth rate	$\mu_{max,NOB}$	(day^{-1})	0.2 – 2.6	(Ahn et al., 2008)
decay rate	b_{NOB}	(day^{-1})	0.08-1.7	(Ahn et al., 2008; Munz et al., 2010)
S_{NO2} half saturation	K_{NO2}	($mg\text{-}N{\cdot}L^{-1}$)	0.05 – 3	(Marsili-Libelli et al., 2001; Jones et al., 2007; Kampschreur et al., 2007)
S_{NO2} yield	Y_{NOB}	($mg\text{-}COD{\cdot}mg\text{-}N^{-1}$)	0.06 – 0.10	(Sin et al., 2008)

Fig. 1. Summary of the two step model utilized in this research to describe nitrification. Shown in the upper box are the five process equations describing the net production rates of ammonia (S_{NH}), AOB, nitrite (S_{NO2}), NOB and nitrate (S_{NO3}) during nitrification. Shown in the bottom boxes are the range of the AOB and NOB model parameters used in the 2000 Monte Carlo simulations (Chandran et al., 2008; Jones et al., 2007; Kampschreur et al., 2007; Manser et al., 2005; Marsili-Libelli et al., 2001; Munz et al., 2010, Munz et al., 2011; Sin et al., 2008).

biodegradation by AOB in the absence of growth; and (iii) biodegradation due to heterotrophs (HET) present in the mixed culture.

$$\frac{dS_{ATN}}{dt} = -\{[\{[T_{ATN-AOB}\mu_{AOB}] + [k_{ATN-AOB}]\}X_{AOB}] + [\{\alpha_{ATN-HET}\}X_{HET}]\}S_{ATN} \quad (2)$$

where $T_{ATN-AOB}$ is the atenolol transformation coefficient linked to AOB growth [$L^3M_{COD}^{-1}$]; μ_{AOB} is the specific AOB growth rate [T^{-1}]; $k_{ATN-AOB}$ is a biomass normalized degradation rate coefficient for atenolol in the absence of AOB growth [$L^3M_{COD}^{-1}T^{-1}$]; X_{AOB} is the AOB concentration [$M_{COD}^3L^{-1}$]; $\alpha_{ATN-HET}$ [$L^3M_{COD}^{-1}T^{-1}$] is the biomass normalized degradation rate coefficient for atenolol by heterotrophic bacteria; X_{HET} is the concentration of heterotrophs [$M_{COD}^3L^{-1}$] which is assumed to be constant over the short duration of experiments (see X_{HET} modeling section in Supplementary Information (SI)); and, S_{ATN} is concentration of atenolol [$M_{ATN}L^{-3}$].

Simulations related to Eq. (2) were conducted by first evaluating $\alpha_{ATN-HET}$. X_{HET} was reported to be 13 mg-COD L^{-1} and held constant while $\alpha_{ATN-HET}$ was fit to the data set in which ammonia oxidation was inhibited (Sathyamoorthy et al., 2013). It should be noted here that this produces a singular value of $\alpha_{ATN-HET}$ as none of the biokinetic parameters varied in the MC analysis are active when ammonia oxidation is inhibited. Each nitrification biokinetic parameter set producing a behavior simulation for the nitrification control reactor are employed with $\alpha_{ATN-HET}$ and X_{HET} to determine best fit values for $T_{ATN-AOB}$ and $k_{ATN-AOB}$ (i.e., by minimizing the SSE between measured and predicted S_{ATN} in the reactors containing atenolol). Uncertainty intervals for atenolol biodegradation are subsequently determined using a protocol identical to that described for the nitrification process with the likelihood function shown as Eq. (3).

$$L_{M-ATN}(\theta_k|Y_k) = \left[\frac{1}{2}\left(1 - \frac{\sigma_{e,A,k}^2}{\sigma_{o,A}^2}\right)\right] + \left[\frac{1}{2}\left(1 - \frac{\sigma_{e,B,k}^2}{\sigma_{o,B}^2}\right)\right] \quad (3)$$

where $\sigma_{e,A,k}^2$ and $\sigma_{e,B,k}^2$ are the variance of the residuals from the replicate experiments A and B for a particular simulation k, and $\sigma_{o,A}^2$ and $\sigma_{o,B}^2$ are the variances of the S_{ATN} values measured in each of the replicate experiments. Behavioral simulations are selected as described above using a selected threshold level (as noted above this threshold tied to NSE and selected to be greater than 0.70). Only the behavioral simulations are used in the subsequent parameter sensitivity analyses.

Parameter sensitivity is assessed by quantifying and comparing elasticity coefficients (ε_i) (Louca, 2007). An elasticity coefficient $\varepsilon_{X/Y}$ is defined as shown in Eq. (4) and represents the percentage change in the model output y corresponding to one percent change in a particular model parameter x.

$$\varepsilon_{X/Y} = \frac{\partial Y/Y}{\partial X/X} \quad (4)$$

In this research, we have used a dimensionless formulation for elasticity (Sankarasubramanian et al., 2001) and estimate elasticity coefficients about the mean value of the behavioral simulations. A detailed derivation of the dimensionless elasticity formulation is provided in the SI. In brief, the total derivative of the model output (dy) was calculated through application of the chain rule utilizing the partial derivative of the model output relative to each model parameter. Due to the nature of the total derivative, this procedure produces a linear relationship between the fractional change in model output and the fractional change in each of the model parameters regardless of the relationship between Y and X. Therefore, no assumptions are required about the underlying form of the model as is normally necessary when estimating elasticities. In the case of the CPB model the resulting relationship between the fractional change in a model output (i.e., $T_{ATN-AOB}$ or $k_{ATN-AOB}$) and fractional changes in each of the biokinetic parameters and elasticities is given by:

$$Y^* = \varepsilon_{\mu_{MAX,AOB}/Y}\mu_{MAX,AOB}^* + \varepsilon_{b_{AOB}/Y}b_{AOB}^* + \varepsilon_{K_{NH}/Y}K_{NH}^* + \varepsilon_{\mu_{MAX,NOB}/Y}\mu_{MAX,NOB}^* + \varepsilon_{b_{NOB}/Y}b_{NOB}^* + \varepsilon_{K_{NO2}/Y}K_{NO2}^* \quad (5)$$

Here the fractional change in the model output is relative to the mean value determined from the behavioral simulations (Y^*). Asterisks in Eq. (5) indicate that quantity is a ratio of the deviation from the mean value to the mean value (see Eq. (6) for an example using $\mu_{MAX,AOB}$, and SI for additional details).

$$\mu_{MAX,AOB,i}^* = \frac{(\mu_{MAX,AOB,i} - \overline{\mu}_{MAX,AOB})}{\overline{\mu}_{MAX,AOB}} \quad (6)$$

The coefficient for each predictor in Eq. (5) are the elasticities, which may be now estimated using multivariate ordinary least-squares (OLS) regression. Recall that the linear structure here results from the chain rule derivation (see SI) and our definition of elasticity (Eq. (4)). It should be noted that other definitions of elasticity may be used which lead to estimation methods which depend on particular model formulations such as a log-log and log-linear models which are used widely to estimate elasticities in economics (Wooldridge, 2008). Another important advantage of our elasticity estimation method is that it results in confidence intervals and hypothesis tests concerning the elasticity estimates as discussed in Section 3.2.

3. Results and discussion

3.1. Monte Carlo analyses and GLUE implementation

3.1.1. Nitrification in absence of pharmaceuticals

Data from two nitrification control experiments were employed herein – those from the control during biodegradation experiments conducted with atenolol (denoted here as set I), and those from the control during biodegradation experiments conducted with sotalol (denoted here as set II). Recall that these control experiments were used to assess nitrification kinetics in the absence of the pharmaceutical as part of an experimental matrix designed to examine the degradation of atenolol or sotalol. It is in this way that these two sets of data provide an insight into how the microbial community in the nitrification enrichment culture was functioning over time, as the data sets were developed 60 days apart.

1994 and 1987 of the 2000 simulations for data sets I and II, respectively, result in $L_M > 0$. Values of $L_M < 0$ suggests that a given set of model parameters results in behavior uncharacteristic of the system and therefore these parameter sets are discarded from further consideration (Beven and Binley, 1992; Chin, 2009). Note that only a small fraction of the total simulations are discarded (i.e., 0.3% and 0.7%, respectively). There is no statistically significant correlation between the posterior distributions of parameters varied in the MC simulations for either data set I (atenolol) or II (sotalol). We also confirmed there is no statistically significant correlation between the parameters and their resulting values of L_M (see Tables S-1 and S-2 in SI). The positive L_M values (1994) for data set I are tightly clustered between 0.91 and 0.99; all but one of the L_M values are greater than 0.91. The median value of L_M for these simulations is 0.96, and the 25th and 75th percentile values are 0.95 and 0.97, respectively. Interestingly, simulations for data set II all produce $L_M < 0.90$. The 1987 positive L_M values for data set II range from 0.13 to 0.85. The median value of L_M is 0.84, and the 25th and 75th percentile values are 0.83 and 0.85, respectively. These metrics suggest that while there are some parameter sets that produce low values of L_M for set II, most simulations are tightly clustered around the median value of 0.84. Recall that the experiments in sets I and II were conducted 60 days apart. We hypothesize that the differences in the distribution of L_M values for data sets I and II may relate to dynamics in the microbial community of the biomass source that were not revealed by the qPCR characterization employed in Sathyamoorthy et al. (2013). Simulations for the nitrification control experiments suggest that the two step nitrification model and a range of biokinetic parameters provide reasonable descriptions of the measured concentrations of nitrogen species.

As noted previously the selection of the behavioral threshold is inherently subjective and is unnecessary when one uses a Bayesian approach to GLUE (Mantovan and Todini, 2006; Stedinger et al., 2008). This suggests that modelers must often compromise between the competing demands of retaining the maximum number of simulations and improving the perceived quality of these simulations through goodness-of-fit metrics. To consider the influence of the behavioral threshold on the number of simulations retained when using GLUE, $L_{M,BEV}$ was varied between 0.70 and 1.00 for sets I and II (Fig. 2). Selection of $L_{M,BEV} = 0.70$, based on the generally accepted criteria for NSE, results in 1993 and 1980 behavioral simulations ($N_{BEH.SIM}$) for data sets I and II, respectively. In fact, for $0.70 \leq L_{M,BEV} \leq 0.95$ the difference in $N_{BEH.SIM}$ is one (i.e., $1993 \geq N_{BEH.SIM} \geq 1992$). It is only when $L_{M,BEV}$ exceeds 0.95 that the number of behavior simulations decreases substantially with increasing $L_{M,BEV}$. For set II, $N_{BEH.SIM}$ remains the same (i.e., 1980) over the range $0.70 \leq L_{M,BEV} \leq 0.82$, but begins to decrease

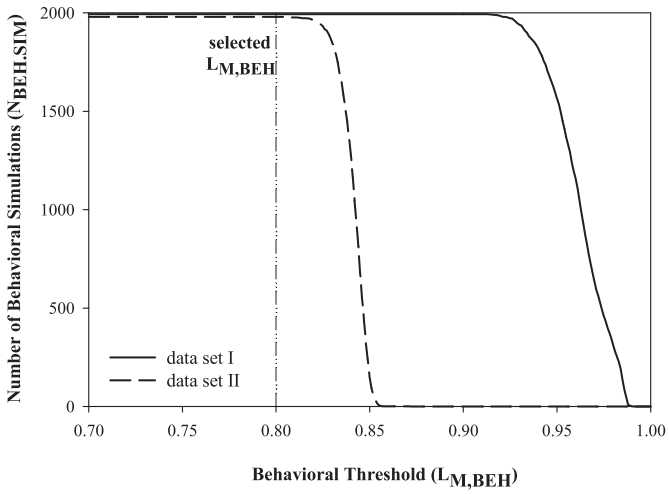

Fig. 2. Reduction in the number of behavioral simulations as a function of the selected behavioral threshold ($L_{M,BEH}$) for data sets I and II. Selected $L_{M,BEH}$ of 0.80 is shown as the vertical line.

substantially if $L_{M,BEV}$ exceeds 0.82. These results suggest that $L_{M,BEV} = 0.82$ produces a similar interpretation of uncertainty to that produced using $L_{M,BEV} = 0.70$ in these nitrification control reactors. The results also demonstrate that a criterion of $L_{M,BEV} = 0.80$, rather than 0.70, may be a more meaningful representation of model performance since L_M is tied back to NSE and larger NSEs indicate better model performance. Thus, we elect to use $L_{M,BEV} = 0.80$ throughout the remaining analyses as this is indicative of good model performance while preserving diversity in the parameter sets (i.e., 1993 and 1980 behavioral simulations for data set I and II, respectively). It is important to note that the evaluation of $L_{M,BEV}$ described here is specific to the Sathyamoorthy et al. (2013) data sets and should not be interpreted as a more general criteria. In fact, the analysis highlights the subjective nature of the behavioral threshold when utilizing GLUE.

Shown in Fig. 3 are the best fit estimates for $X_{AOB,t0}$ and $X_{NOB,t0}$ produced using the behavioral MC simulations for data sets I and II. Estimates of the AOB and NOB biomass concentrations (and ratios) obtained in the behavioral simulations are compared to those obtained from quantitative real time polymerase chain reaction (qPCR) in Sathyamoorthy et al. (2013). Interestingly in both experiments, the qPCR values for X_{AOB} fall in the range of 80th to 90th percentile, while the values for X_{NOB} are at the 55th percentile. It should be noted here that order-of-magnitude variability in biomass concentrations obtained using qPCR is commonly acknowledged (Harms et al., 2003; Ahn et al., 2008).

3.1.2. Nitrification in presence of pharmaceuticals

Parameter sets that produced behavioral simulations ($L_{M,BEV} = 0.80$) in the nitrification controls (i.e., in the absence of pharmaceutical) were employed to generate 5th and 95th uncertainty intervals for the predictions of ammonia oxidation when either atenolol or sotalol was present at 15 μg/L (Fig. 4). We refer to these behavioral simulations as the base case (no inhibition) model. For sotalol the uncertainty intervals generated using this informal GLUE approach are shown to generally enclose the measured concentrations of ammonia. Results for atenolol are more complicated. Here the uncertainty bands generated using the informal GLUE approach well enclose the ammonia data so long as ammonia concentrations remain high (i.e., substantially greater than K_s). However, as ammonia concentrations decrease the measured concentrations fall ever increasingly outside of the uncertainty intervals generated for these model predictions (Fig. 4, base case). Thus, there appears to be errors that are unaccounted for in the case of atenolol model predictions. We know from our laboratory experiments that atenolol (unlike sotalol) competitively inhibits ammonia oxidation (Sathyamoorthy et al., 2013). Thus the inability of GLUE to generate meaningful uncertainty intervals over the range of ammonia concentrations most strongly influenced by the inhibition suggests model error may be the source of the additional error. This observation has important practical significance, since many biological treatment processes are conducted in reactors having relatively low ammonia concentrations (i.e., CSTRs designed for nutrient management).

We explored the influence of model error by reassessing the nitrification data from the atenolol experiments with an AOB growth rate that accounts for competitive inhibition as shown in Eq. (7) (Bailey and Ollis, 1986).

Quantile	X_{AOB}	X_{NOB}	X_{NOB}/X_{AOB}
5th	17	6	0.12
50th	29	15	0.51
95th	99	68	2.44

Quantile	X_{AOB}	X_{NOB}	X_{NOB}/X_{AOB}
5th	14	5	0.09
50th	24	10	0.39
95th	85	44	2.05

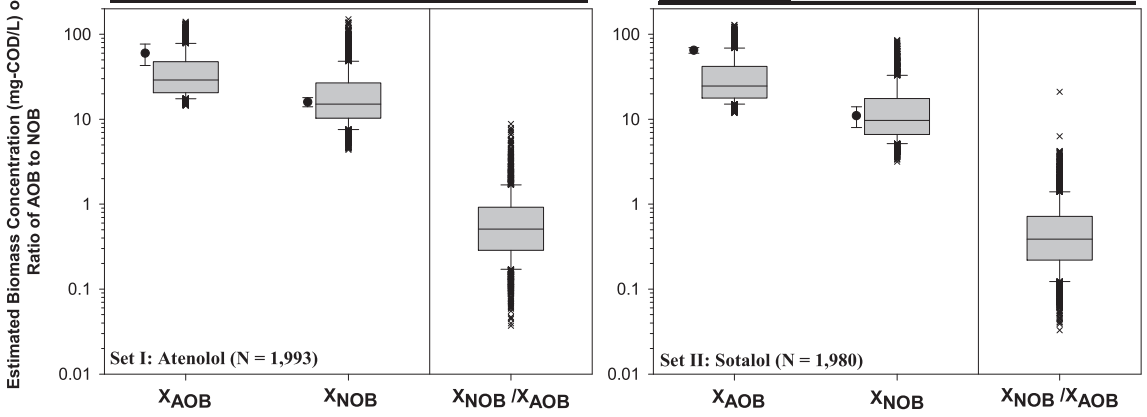

Fig. 3. Biomass concentrations and ratios estimated from the behavioral MC simulations for data sets I (left) and II (right). Estimated biomass concentrations using qPCR from Sathyamoorthy et al. (2013) are shown for comparison to the estimates from the behavioral simulations. Provided in the overlying tables are 5th, 50th and 95th percentile values of each concentration and ratio.

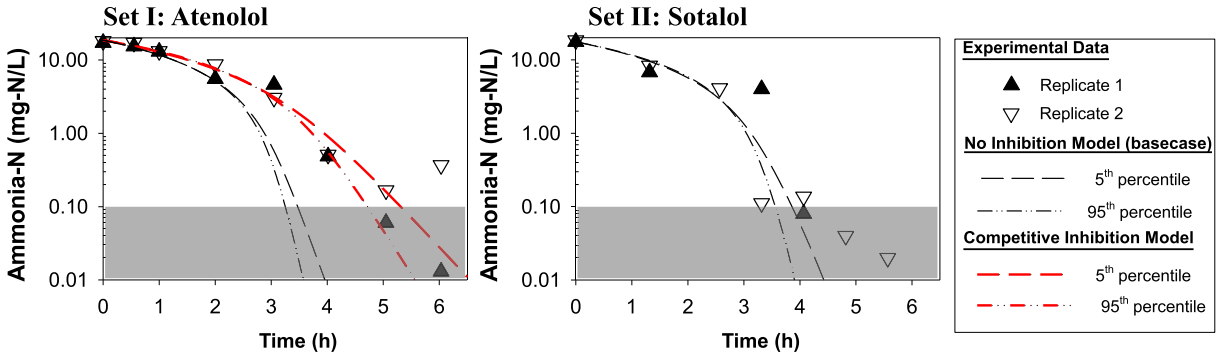

Fig. 4. Uncertainty intervals generated using GLUE for ammonia concentrations during ammonia oxidation in the presence of atenolol (left) and sotalol (right). Uncertainty intervals were obtained using GLUE with the base case (no inhibition, black) and competitive inhibition models (red). Also shown are the measured ammonia concentrations for each experimental replicate. (For interpretation of the references to color in this figure legend, the reader is referred to the web version of this article.)

$$r_{G,X_{AOB}} = \left[\mu_{MAX,AOB}\left(\frac{S_{NH}}{K_{NH}\left(1+\frac{S_{ATN}}{K_{I,ATN-AOB}}\right)+S_{NH}}\right)\right]X_{AOB} \quad (7)$$

Note the use of Eq. (7) introduces a new parameter, $K_{I,ATN-AOB}$ that cannot be independently evaluated using the data sets of Sathyamoorthy et al. (2013). Thus, $K_{I,ATN}$ must be fit to the nitrification data of the replicate atenolol experiments. Fitting $K_{I,ATN}$ in the competitive inhibition growth equation for AOB (Eq. (7)) enables development of uncertainty intervals based on the fitted competitive inhibition model. Thus, our approach here is to compare the 5th and 95th percentile uncertainty intervals produced using behavioral simulations when implementing the competitive inhibition model with those produced from the behavioral simulations when the base-case model (i.e., no inhibition model) is implemented. If model structural errors are accounted for by GLUE as is often the claim (e.g., Beven and Freer, 2001), the uncertainty intervals for these models should be similar.

We assess the uncertainty in models resulting from use of the competitive-inhibition hypothesis using the modified likelihood function (L_{M2}) in GLUE. L_{M2} is based upon equally weighting the two replicate reactors (A and B) when considering S_{NH}, S_{NO2}, and S_{NO3} as shown in Eq. (8).

$$L_{M2}(\theta_k|Y_k) = \left[0.5^*\sum_i \omega_i\left(1-\frac{\sigma^2_{e,A,i,k}}{\sigma^2_{o,A,i}}\right)\right] + \left[0.5^*\sum_i \omega_i\left(1-\frac{\sigma^2_{e,B,i,k}}{\sigma^2_{o,B,i}}\right)\right] \quad i = S_{NH}, S_{NO2}, S_{NO3} \quad (8)$$

Here σ_e is the variance of the residuals and σ_o is the variance of the measured values. The NSE values of each of the nitrogen species are equally weighted (i.e., $\omega_i = 1/3$). The subscripts A and B refer to each of the experimental replicates. The behavioral threshold for the likelihood function utilized in this analysis (Eq. (8)) is denoted $L_{M2,BEV}$, and set to 0.80 to be consistent with the analysis in the absence of the pharmaceutical (section 3.1.1). The efficacy of the base-case and competitive-inhibition models in describing the measured concentrations of nitrogen species over the course of the experiments are compared using the small-sample Akaike Information Criteria (AIC_C, Eq. (9)) (Akaike, 1973, 1974; Burnham and Anderson, 2002).

$$AIC_C = \left[n\cdot\ln\left(\frac{SSE}{n}\right)+2K\right]+\frac{2K(K+1)}{(n-K-1)} \quad (9)$$

Here n is the sample size, SSE is the sum of square errors, K is the number of estimated model parameters which includes the number of fitted model parameters (P) and one model variance parameter (i.e., $K = P + 1$). AIC_c ranks the ability of competing models to explain the data after imposing a penalty for inclusion of additional model parameters and simultaneously provides a trade-off between bias and variance (Hurvich and Tsai, 1991). AIC_C values are not bounded and the model producing the lowest AIC_C value is chosen. An AIC_C difference of greater than 10 suggests that the worse model (with the higher AIC_C) is not supported by the data (Burnham and Anderson, 2002).

Implementation of the competitive inhibition model lowers the AIC_C for the behavioral simulations suggesting that the data support the use of the competitive inhibition model over the base-case (no-inhibition) model (Table 1). These reductions in AICc specifically result from better simulation of the ammonia data (see SSE and AICc for S_{NH} in Table 1, and Fig. 4). Competitive inhibition of ammonia oxidation results in an increase in the effective half saturation coefficient by the ratio of the atenolol concentration (S_{ATN}) to the inhibition coefficient ($K_{I,ATN}$) (see Eq. (8)). As shown in Fig. 4, the uncertainty intervals determined using GLUE with the competitive inhibition model enclose the full range of measured concentrations of ammonia, as they should when the model is correctly specified. Thus, in this instance, use of GLUE (i.e., with an accurate model of ammonia oxidation) appears to be an effective

Table 1
Comparison of GLUE likelihood function L_{M2} and goodness of fit metrics when using a Monod model for AOB growth (no inhibition) versus competitive inhibition model for the combined data sets from experimental reactors with atenolol.

Metric	Quantile	No inhibition	Competitive inhibition
$N_{BEH,SIM}$		1993	1970
Metrics with all measured nitrogen species (S_{NH}, S_{NO2}, S_{NO3})			
L_{M2}	5th	0.79	0.82
	50th	0.81	0.84
	95th	0.85	0.86
SSE	5th	30.39	19.29
	50th	31.32	20.55
	95th	32.11	23.04
AIC_C	5th	12.86	4.87
	50th	13.59	6.38
	95th	14.18	9.13
Metrics with only ammonia-N (S_{NH})			
SSE	5th	11.06	5.68
	50th	11.40	6.13
	95th	11.56	7.13
AIC_C	5th	−11.39	−24.48
	50th	−10.68	−22.65
	95th	−10.33	−19.04

tool to generate uncertainty bounds. Collectively, these results highlight the importance of accurate model selection when using GLUE for uncertainty analysis.

3.2. Parameter sensitivity analysis

$T_{ATN-AOB}$ and $k_{ATN-AOB}$ are estimated in each of the 1970 behavioral simulations obtained using the competitive-inhibition model. All of these simulations are also behavioral when considering L_{M-PhAC} as all L_{M-PhAC} values are greater than 0.95. The high values of L_{M-PhAC} indicate the simulations using CPB are extremely good representations of the PhAC data. Values of $T_{ATN-AOB}$ and $k_{ATN-AOB}$ are weakly correlated with each other ($R = 0.33$). The ranges of these parameters are $63.8 \leq T_{ATN-AOB} \leq 74.8$ L.g-COD^{-1} and $5.6 \leq k_{ATN-AOB} \leq 52.7$ L g-COD^{-1} d^{-1}.

Shown in Table 2 are the elasticity estimates for $T_{ATN-AOB}$, $k_{ATN-AOB}$ and $K_{I,ATN-AOB}$ based on the parameter sets and estimates in the 1970 behavioral simulations. All estimated elasticities obtained are statistically significant at the 0.05-level, unless otherwise noted. Significance levels for these elasticity estimates are based on the well-known *t*-tests associated with multivariate linear regression, another attractive feature and benefit of our nonparametric elasticity estimation method. Also provided for each parameter is the standard error and percentage of the model sum of square errors attributable to its elasticity. The goodness of fit of each of the elasticity models is indicated using the NSE, in lieu of the coefficient of determination (R^2), as these are no-intercept models, in which case, R^2 lacks meaning. Model residuals associated with Eq. (5) were found to be well approximated by a homoscedastic normal distribution.

The high values of NSE suggest that the total derivative defined in Eq. (S2) effectively captures the parameters contributing to the variation in $T_{ATN-AOB}$, $k_{ATN-AOB}$ and $K_{I,ATN-AOB}$. In fact, variances in $T_{ATN-AOB}$, $k_{ATN-AOB}$ and $K_{I,ATN-AOB}$ are nearly explained by the AOB biokinetic parameters alone (see %model SSEs in Table 2), suggesting NOB biokinetic parameters contribute little sensitivity to these parameters. This is not surprising as $T_{ATN-AOB}$, $k_{ATN-AOB}$ and $K_{I,ATN-AOB}$ all relate to ammonia oxidation, not nitrite oxidation.

The elasticities shown in Table 2 suggest that small deviations in $T_{ATN-AOB}$ (coefficient of variation of $T_{ATN-AOB} = 3\%$) are primarily linked to deviations in b_{AOB} through a weak inverse relationship ($\varepsilon_{b_{AOB}/T_{ATN-AOB}} = -0.06$). $T_{ATN-AOB}$, however, is sensitive the AOB net growth rate (i.e., all three AOB growth parameters) which corresponds to the physical interpretation of $T_{ATN-AOB}$ as representing atenolol cometabolism during AOB growth. In contrast, deviations in $k_{ATN-AOB}$ appear related to deviations in $\mu_{MAX,AOB}$ ($\varepsilon_{\mu_{MAX-AOB}-k_{ATN-AOB}} = 0.95$). We hypothesize that the sensitivity of $k_{ATN-AOB}$ to $\mu_{MAX,AOB}$ results from the fact $k_{ATN-AOB}$ controls the model fit after ammonia oxidation is complete. That is, higher $\mu_{MAX,AOB}$ results in faster completion of ammonia oxidation, and consequently greater influence of $k_{ATN-AOB}$. Deviations in the AOB growth inhibition coefficient ($K_{I,ATN-AOB}$) are well explained by deviations in K_{NH} ($\varepsilon_{K_{NH}-K_{I,ATN-AOB}} = 0.92$, see Table 2) given that $K_{I,ATN-AOB}$ effectively increases K_{NH} (Eq. (7)). While this may appear to suggest there is a less pronounced inhibitory effect for larger values of K_{NH}, it is important to recognize that the range of $K_{I,ATN-AOB}$ values reported here is similar to the range of environmentally relevant concentrations of atenolol (<10 μg L^{-1}).

4. Conclusions and implications

The application of GLUE using an informal likelihood function for constructing uncertainty intervals associated with model simulations of nitrification has been evaluated in this research. Our findings suggest that uncertainty intervals based on GLUE for nitrification models, in cases where parameter uncertainty is the primary source of errors, appear to satisfactorily encompass experimental data and in this instance provide a good estimate of the uncertainty resulting from parameter uncertainty alone. However, where model structural errors may arise due to inhibition, GLUE cannot produce uncertainty intervals large enough to explain variations in model output which we have observed. These results strongly suggest that where an inappropriate model basis is used to develop uncertainty intervals, GLUE, used as prescribed, is incapable of producing meaningful estimates of model uncertainty. We consider this to be a particularly important finding as GLUE continues to gain popularity in the wastewater treatment process modeling community. Epistemic uncertainty due a range of factors including changing influent quality or potential influx of inhibitory pollutants, are commonplace in wastewater treatment plants. Therefore, from the perspective of wastewater treatment process modeling, our results suggest that caution should be exercised when using GLUE with an informal likelihood function to develop uncertainty intervals pertaining to the effectiveness of treatment.

It is worth reiterating that the development of a formal likelihood function for this analysis was made impracticable by the complexity observed in the stochastic structure of the model residuals. This is very often the case for models describing complex phenomena (Liu and Gupta, 2007). Thus, our analysis cannot and does not reflect the full uncertainty associated with particular model output (Stedinger et al., 2008). The use of an informal likelihood function cannot produce prediction intervals which accurately enclose future model predictions. While it may continue to be common practice to use GLUE without a formal likelihood function, we recommend that future research more fully evaluate the structure of model residuals. Such research may result in approximations of a formal likelihood function that support development of meaningful prediction intervals using GLUE.

The multivariate elasticity approach introduced to assess model sensitivity is based on the chain rule which results in a multivariate

Table 2
Elasticity coefficients (ε_i) of biokinetic parameters for atenolol biodegradation parameters using estimated values from 1970 behavioral simulations employing the competitive inhibition model for AOB growth.

	Elasticity Values (with Standard Errors); % of Model Sum of Square Errors Explained by Each Elasticity Term						Model NSE
	$\varepsilon_{\mu_{MAX-AOB}}$	$\varepsilon_{b_{AOB}}$	$\varepsilon_{K_{NH}}$	$\varepsilon_{\mu_{MAX-NOB}}$	$\varepsilon_{b_{NOB}}$	$\varepsilon_{K_{NO2}}$	
$T^*_{ATN-AOB}$	0.030 (0.000) 20.6%	−0.056 (0.000) 64.5%	0.020 (0.000) 12.2%	0.000 (0.000) 0%	−0.001 (0.000) 0%	−0.009 (0.000) 2.6%	0.991
$k^*_{ATN-AOB}$	0.945 (0.001) 97.1%	0.090 (0.002) 0.8%	−0.108 (0.001) 1.6%	*N/A ($p > 0.05$)*	*N/A ($p > 0.05$)*	0.006 (0.001) 0%	0.995
$K^*_{I,ATN-AOB}$	−0.010 (0.002) 0.1%	0.013 (0.002) 0%	0.924 (0.001) 98.8%	−0.006 (0.001) 0%	0.005 (0.001) 0%	0.072 (0.001) 0.7%	0.996

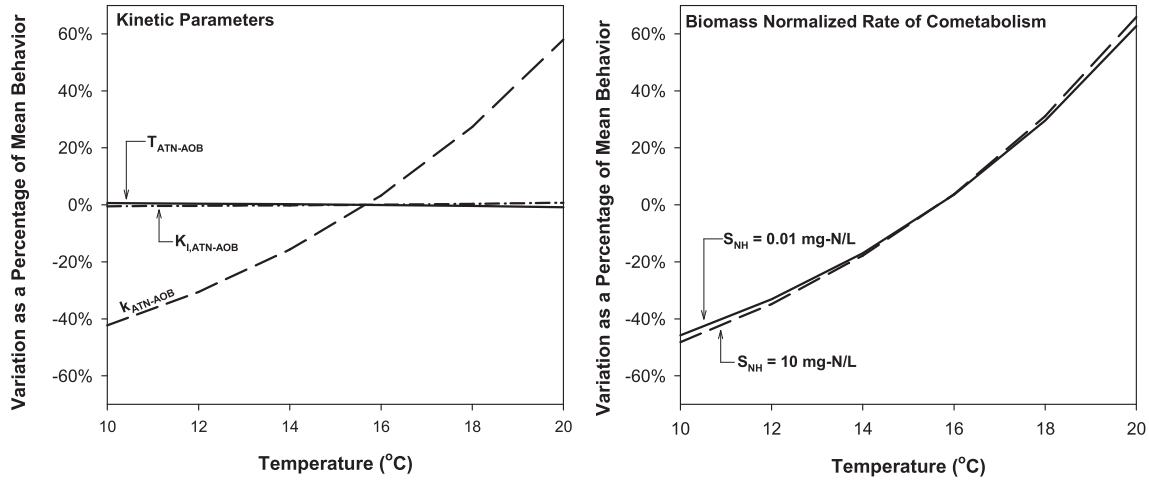

Fig. 5. Influence of wastewater temperature on the biodegradation of atenolol. Variation of kinetic parameters (left) and rate of cometabolic biodegradation by AOB (right). The rate plot assumes 1 μg/L atenolol, though it should be noted that atenolol concentration only influences the variation in rate through AOB inhibition.

linear model, regardless of the form of the original model of interest. Thus our approach enables the use of multivariate linear regression for estimation of model parameter elasticities (sensitivity) along with statistical inference such as confidence intervals and hypothesis tests. This method is unique because it can handle multivariate elasticities, yet it is completely nonparametric in the sense that it does not require any model assumptions (see SI) for its derivation and/or use. Results from the sensitivity analysis suggest that the cometabolic transformation coefficient for atenolol biodegradation linked to AOB growth is relatively inelastic to AOB biokinetics. On the other hand, the non-growth related transformation coefficient is elastic. Quantification of these elasticities has important implications for understanding PhAC biodegradation by AOB in WWTPs. Principally, it allows utilization of lab-derived biodegradation coefficients when attempting to characterize PhAC biodegradation in full-scale systems. As an example, we consider here the influence of 10 °C fluctuation in water temperature (e.g., seasonal variation) on the degradation of atenolol by AOB in a WWTP. We estimated the variation in $T_{ATN-AOB}$, $k_{ATN-AOB}$ and $K_{I,ATN-AOB}$ using AOB and NOB biokinetics and the temperature dependencies proposed by Manser et al. (2006) and Kaelin et al. (2009) (see Table S-3 in SI). The analysis suggests that $T_{ATN-AOB}$ and $K_{I,ATN-AOB}$ are insensitive to temperature (Fig. 5, left). In contrast, $k_{ATN-AOB}$ varies significantly over the 10 °C range in temperature. The variation in $k_{ATN-AOB}$ with temperature is a direct result of the variation in $\mu_{MAX,AOB}$ in this scenario. The influence of this variation in $k_{ATN-AOB}$ is shown by considering the change in the rate of cometabolism (due to temperature effects) relative to the mean rate of cometabolism for this range in temperature. This metric is shown in Fig. 5 (right) for conditions indicative of WWTPs that produce: (a) near complete nitrification ($S_{NH} = 0.01$ mg-N/L); and, (b) a near incomplete nitrification ($S_{NH} = 10$ mg-N/L). In both cases the atenolol concentration is assumed to be 1 μg/L, although this only influences the variation in the rate through the inhibition of AOB. This simplified analysis suggests that changes in temperature may result in large variations to the rate of atenolol cometabolism by AOB (Fig. 5, right). Interestingly, the degree of nitrification has minimal influence on variations in atenolol degradation due to temperature changes. Future research is warranted to assess these model based findings through laboratory experiments. Thus, the ability to maintain nitrification will only impart substantial variations in the rate of cometabolism when AOB biomass concentrations begin to fluctuate (which is not accounted for in these simplified simulations). To our knowledge this is the first evaluation of temperature related sensitivity of PhAC biodegradation in biological wastewater treatment processes. It is important to recall that elasticities developed herein are specific to the range of parameter values utilized in the MC simulations. While the selected parameter ranges utilized in the MC simulations are representative of most nitrification processes (see Fig. 1), care should be taken to reassess elasticities for outlying biokinetic behavior observed in a natural or engineered process.

Acknowledgments

Partial support was provided by the Massachusetts Water Resources Research Center under grant number 2011MA291B. Additional support was provided by Tufts University in the form of Faculty Research Awards Committee grant to C.A.R, and a Graduate Student Award to S.S. We are also grateful to three anonymous reviewers who helped improve this manuscript. Any opinions, findings, and conclusions or recommendations expressed in this material are those of the authors and do not necessarily reflect the views of the sponsors.

Appendix A. Supplementary material

Supplementary material related to this article can be found at http://dx.doi.org/10.1016/j.envsoft.2014.06.006.

References

Abramowitz, G., Gupta, H., Pitman, A., Wang, Y.P., Leuning, R., Cleugh, H., Hsu, K.L., 2006. Neural error regression diagnosis (NERD): a tool for model bias identification and prognostic data assimilation. J. Hydrometeorol. 7 (1), 160–177.
Ahn, J.H., Yu, R., Chandran, K., 2008. Distinctive microbial ecology and biokinetics of autotrophic ammonia and nitrite oxidation in a partial nitrification bioreactor. Biotechnol. Bioeng. 100 (6), 1078–1087.
Akaike, H., 1973. In: Csáki, F., Petrov, B.N. (Eds.), Information Theory and an Extension of the Maximum Likelihood Principle. Akademiai Kiado, Budapest, Hungary, pp. 267–281.
Akaike, H., 1974. A new look at the statistical model identification. IEEE Trans. Automat. Control 19 (6), 716–723.
Bailey, J.E., Ollis, D.F., 1986. Biochemical Engineering Fundamentals. McGraw-Hill.
Belia, E., Amerlinck, Y., Benedetti, L., Johnson, B., Sin, G., Vanrolleghem, P.A., Gernaey, K.V., Gillot, S., Neumann, M.B., Rieger, L., Shaw, A., Villez, K., 2009. Wastewater treatment modelling: dealing with uncertainties. Water Sci. Technol. 60 (8), 1929–1941.

Benedetti, L., Claeys, F., Nopens, I., Vanrolleghem, P.A., 2011. Assessing the convergence of LHS Monte Carlo simulations of wastewater treatment models. Water Sci. Technol. 63 (10), 2219–2224.
Beven, K., Binley, A., 1992. The future of distributed models – model calibration and uncertainty prediction. Hydrol. Process 6 (3), 279–298.
Beven, K., Freer, J., Hankin, B., Schulz, K., 2000. The use of generalized likelihood measures for uncertainty estimation in high-order models of environmental systems. In: Fitzgerald, W.J., Smith, R.L., Walden, A.T., Young, P.C. (Eds.), Nonlinear and Nonstationary Signal Processing. Cambridge Univ. Press, Cambridge, UK, pp. 115–151.
Beven, K., Freer, J., 2001. Equifinality, data assimilation, and uncertainty estimation in mechanistic modelling of complex environmental systems using the GLUE methodology. J. Hydrol. 249, 11–29.
Beven, K.J., Smith, P.J., Freer, J., 2008. So just why would a modeller choose to be incoherent? J. Hydrol 354 (1–4), 15–32.
Burnham, K.P., Anderson, D.R., 2002. Model Selection and Multimodel Inference: A Practical Information-theoretic Approach. Springer-Verlag, New York.
Carrera, J., Neuman, S.P., 1986. Estimation of aquifer parameters under transient and steady-state conditions 3. Application to synthetic and field data. Water Resour. Res. 22 (2), 228–242.
Chandran, K., Hu, Z.Q., Smets, B.F., 2008. A critical comparison of extant batch respirometric and substrate depletion assays for estimation of nitrification biokinetics. Biotechnol. Bioeng. 101 (1), 62–72.
Chandran, K., Smets, B.F., 2000. Single-step nitrification models erroneously describe batch ammonia oxidation profiles when nitrite oxidation becomes rate limiting. Biotechnol. Bioeng. 68 (4), 396–406.
Chiew, F.H.S., 2006. Estimation of rainfall elasticity of streamflow in Australia. Hydrol. Sci. J. 51 (4), 613–625.
Chin, D.A., 2009. Predictive uncertainty in water-quality modeling. J. Environ. Eng. ASCE 135 (12), 1315–1325.
Cosenza, A., Mannina, G., Neumann, M.B., Viviani, G., Vanrolleghem, P.A., 2013. Biological nitrogen and phosphorus removal in membrane bioreactors: model development and parameter estimation. Bioproc. Biosyst. Eng. 36 (4), 499–514.
Criddle, C.S., 1993. The Kinetics of Cometabolism. Biotechnol. Bioeng. 41 (11), 1048–1056.
Di Bella, G., Mannina, G., Viviani, G., 2008. An integrated model for physical-biological wastewater organic removal in a submerged membrane bioreactor: model development and parameter estimation. J. Mem. Sci. 322 (1), 1–12.
Fell, D.A., 1992. Metabolic control analysis - a survey of its theoretical and experimental development. Biochem. J. 286, 313–330.
Flores-Alsina, X., Corominas, L., Neumann, M.B., Vanrolleghem, P.A., 2012. Assessing the use of activated sludge process design guidelines in wastewater treatment plant projects: A methodology based on global sensitivity analysis. Environ. Modell. Softw. 38, 50–58.
Flores-Alsina, X., Rodriguez-Roda, I., Sin, G., Gernaey, K.V., 2008. Multi-criteria evaluation of wastewater treatment plant control strategies under uncertainty. Water Res. 42 (17), 4485–4497.
Freer, J., Beven, K., Ambroise, B., 1996. Bayesian estimation of uncertainty in runoff prediction and the value of data: an application of the GLUE approach. Water Resour. Res. 32 (7), 2161–2173.
Harms, G., Layton, A.C., Dionisi, H.M., Gregory, I.R., Garrett, V.M., Hawkins, S.A., Robinson, K.G., Sayler, G.S., 2003. Real-time PCR quantification of nitrifying bacteria in a municipal wastewater treatment plant. Environ. Sci. Technol. 37 (2), 343–351.
Henze, M., Grady, C.P.L., Gujer, W., Marais, G.V.R., Matsuo, T., 1987. A general model for single-sludge wastewater treatment systems. Water Res. 21 (5), 505–515.
Henze, M., Gujer, W., Mino, T., Loosdrecht, M.V., 2000. Activated Sludge Models ASM1, ASM2, ASM2d and ASM3. IWA Pub, London.
Hiatt, W.C., Grady, C.P.L., 2008. An updated process model for carbon oxidation, nitrification, and denitrification. Water Environ. Res. 80 (11), 2145–2156.
Hornberger, G.M., Spear, R.C., 1981. An approach to the preliminary analysis of environmental systems. J. Environ. Manage. 12 (1), 7–18.
Hurvich, C.M., Tsai, C.L., 1991. Bias of the corrected AIC criterion for underfitted regression and time series models. Biometrika 78 (3), 499–509.
Jones, R.M., Dold, P., Takacs, I., Chapman, K., Wett, B., Murthy, S., O'Shaughnessy, M., 2007. Simulation for Operation and Control of Reject Water Treatment Processes. Water Environment Federation, San Diego, CA.
Kaelin, D., Manser, R., Rieger, L., Eugster, J., Rottermann, K., Siegrist, H., 2009. Extension of ASM3 for two-step nitrification and denitrification and its calibration and validation with batch tests and pilot scale data. Water Res. 43 (6), 1680–1692.
Kampschreur, M.J., Picioreanu, C., Tan, N., Kleerebezem, R., Jetten, M.S.M., van Loosdrecht, M.C.M., 2007. Unraveling the source of nitric oxide emission during nitrification. Water Environ. Res. 79 (13), 2499–2509.
Liu, Y.Q., Gupta, H.V., 2007. Uncertainty in hydrologic modeling: toward an integrated data assimilation framework. Water Resour. Res. 43 (7).
Louca, F., 2007. Years of High Econometrics. Routledge, London.
Mannina, G., Cosenza, A., Vanrolleghem, P.A., Viviani, G., 2011. A practical protocol for calibration of nutrient removal wastewater treatment models. J. Hydroinfrom. 13 (4), 575–595.
Mannina, G., Cosenza, A., Viviani, G., 2012. Uncertainty assessment of a model for biological nitrogen and phosphorus removal: application to a large wastewater treatment plant. Phys. Chem. Earth 42–44, 61–69.
Mannina, G., Di Bella, G., Viviani, G., 2010. Uncertainty assessment of a membrane bioreactor model using the GLUE methodology. Biochem. Eng. J. 52 (2–3), 263–275.
Manser, R., Gujer, W., Siegrist, H., 2005. Consequences of mass transfer effects on the kinetics of nitrifiers. Water Res. 39 (19), 4633–4642.
Manser, R., Gujer, W., Siegrist, H., 2006. Decay processes of nitrifying bacteria in biological wastewater treatment systems. Water Res. 40 (12), 2416–2426.
Mantovan, P., Todini, E., 2006. Hydrological forecasting uncertainty assessment: incoherence of the GLUE methodology. J. Hydrol. 330 (1–2), 368–381.
Marsili-Libelli, Ratini P., Spagni, A., Bortone, G., 2001. Implementation, study and calibration of a modified ASM2d for the simulation of SBR processes. Water Sci. Technol. 43 (3), 69–76.
McCuen, R.H., Knight, Z., Cutter, A.G., 2006. Evaluation of the Nash-Sutcliffe efficiency index. J. Hydrol. Eng. 11 (6), 597–602.
McKay, M.D., Beckman, R.J., Conover, W.J., 1979. A comparison of three methods for selecting values of input variables in the analysis of output from a computer code. Technometrics 21 (2), 239–245.
Moriasi, D.N., Arnold, J.G., Van Liew, M.W., Bingner, R.L., Harmel, R.D., Veith, T.L., 2007. Model evaluation guidelines for systematic quantification of accuracy in watershed simulations. Trans. ASABE 50 (3), 885–900.
Munz, G., Lubello, C., Oleszkiewicz, J.A., 2011. Factors affecting the growth rates of ammonium and nitrite oxidizing bacteria. Chemosphere 83 (5), 720–725.
Munz, G., Mori, G., Vannini, C., Lubello, C., 2010. Kinetic parameters and inhibition response of ammonia- and nitrite-oxidizing bacteria in membrane bioreactors and conventional activated sludge processes. Environ. Technol. 31 (14), 1557–1564.
Renard, B., Kavetski, D., Kuczera, G., Thyer, M., Franks, S.W., 2010. Understanding predictive uncertainty in hydrologic modeling: the challenge of identifying input and structural errors. Water Resour. Res. 46 (5), W05521.
Rieger, L., Gillot, S., Langergraber, G., Ohtsuki, T., Shaw, A., Takacs, I., Winkler, S., 2013. Guidelines for Using Activated Sludge Models. IWA Publishing, London.
Sankarasubramanian, A., Vogel, R.M., Limbrunner, J.F., 2001. Climate elasticity of streamflow in the United States. Water Resour. Res. 37 (6), 1771–1781.
Sathyamoorthy, S., Chandran, K., Ramsburg, A., 2013. Biodegradation and cometabolic modeling of selected beta blockers during ammonia oxidation. Environ. Sci. Technol. 47 (22), 12835–12843.
Sin, G., Kaelin, D., Kampschreur, M.J., Takacs, I., Wett, B., Gernaey, K.V., Rieger, L., Siegrist, H., van Loosdrecht, M.C.M., 2008. Modelling nitrite in wastewater treatment systems: a discussion of different modelling concepts. Water Sci. Technol. 58 (6), 1155–1171.
Sin, G., Van Hulle, S.W.H., De Pauw, D.J.W., van Griensven, A., Vanrolleghem, P.A., 2005. A critical comparison of systematic calibration protocols for activated sludge models: a SWOT analysis. Water Res. 39 (12), 2459–2474.
Stedinger, J.R., Vogel, R.M., Lee, S.U., Batchelder, R., 2008. Appraisal of the generalized likelihood uncertainty estimation (GLUE) method. Water Resour. Res. 44 (12), W00B06.
Tian, Y., Booij, M.J., Xu, Y.P., 2014. Uncertainty in high and low flows due to model structure and parameter errors. Stoch. Environ. Res. Risk A 28 (2), 319–332.
Vezzaro, L., Eriksson, E., Ledin, A., Mikkelsen, P.S., 2012. Quantification of uncertainty in modelled partitioning and removal of heavy metals (Cu, Zn) in a stormwater retention pond and a biofilter. Water Res. 46 (20), 6891–6903.
Vezzaro, L., Mikkelsen, P.S., 2012. Application of global sensitivity analysis and uncertainty quantification in dynamic modelling of micropollutants in stormwater runoff. Environ. Modell. Softw. 27–28, 40–51.
Vrugt, J.A., ter Braak, C.J.F., Gupta, H.V., Robinson, B.A., 2009. Equifinality of formal (DREAM) and informal (GLUE) Bayesian approaches in hydrologic modeling? Stoch. Environ. Res. Risk A 23 (7), 1011–1026.
Wooldridge, J.M., 2008. Introductory Econometrics A Modern Approach. South-Western Cengage Learning.